

# Identification of 12Cys $\beta$ on tubulin as the binding site of tubulyzine

Yeoun Jin Kim,<sup>a</sup> Dan L. Sackett,<sup>b</sup> Matthieu Schapira,<sup>c,†</sup> Daniel P. Walsh,<sup>d</sup>  
Jaeki Min,<sup>d</sup> Lewis K. Pannell<sup>a</sup> and Young-Tae Chang<sup>d,\*</sup>

<sup>a</sup>National Institute of Diabetes, Digestive, Kidney Diseases, National Institutes of Health, U.S. Department of Health and Human Services, Bethesda, MD 20892, USA

<sup>b</sup>National Institute of Child Health and Human Development, National Institutes of Health, U.S. Department of Health and Human Services, Bethesda, MD 20892, USA

<sup>c</sup>Department of Pharmacology, New York University Medical Center, New York, NY 10016, USA

<sup>d</sup>Department of Chemistry, New York University New York, NY 10003, USA

Received 9 September 2005; revised 24 September 2005; accepted 26 September 2005  
Available online 2 November 2005

**Abstract**—We have undertaken quantitative binding site studies in order to identify the binding site of the known microtubule destabilizing agents, the tubulyzines, in the tubulin dimer. Two different approaches were employed that utilized the tubulyzines and their derivatives. The first approach was based on a chemical affinity labeling method using tubulyzine affinity derivatives, and the second approach employed the mass spectrometric measurement of the differential reactivity of cysteines using the tubulyzines and monobromobimane. Based on overlapping data from these two approaches, we propose that the tubulyzines bind at the guanosine-5'-triphosphate binding site of  $\beta$ -tubulin. Interestingly, we also show that the tubulyzines' binding to tubulin induces a conformational change in tubulin that prevents further interaction of the 239Cys $\beta$  with other reagents.

© 2005 Elsevier Ltd. All rights reserved.

## 1. Introduction

Tubulin, the building block of microtubules, is one of the proven targets for anticancer drugs. Thus far, several agents have been developed that either stabilize or destabilize microtubules, such as taxol and the vinca alkaloids, respectively. Although these agents are currently being used in cancer treatment, problems associated with the intrinsic toxicity and solubility of the known

drugs have prompted the need for the development of improved therapeutics.<sup>1–4</sup> A purine based microtubule inhibitor, myoseverin, has demonstrated unique and promising properties, the most interesting of which is low cytotoxicity.<sup>5,6</sup> Despite the promise of myoseverin, its moderate activity remains to be improved. However, due to synthetic restraints stemming from its purine scaffold, large scale diversity generation and scale-up are difficult. Therefore, we designed a library of tubulin targeted myoseverin derivatives around the triazine scaffold. Its threefold symmetry, low cost, and synthetic flexibility allowed for the generation of diverse, highly pure libraries. We previously identified the microtubule destabilizing entities, the tubulyzines, which were shown to target tubulin and possess an activity greater than that of myoseverin itself.<sup>7</sup> Figure 1 shows the structures of myoseverin and its related compounds tubulyzine A and tubulyzine B.

Compared to other tubulin targeting compounds, the unique characteristics of myoseverin and tubulyzine may either come from targeting a different binding site on tubulin or from the existence of cellular targets other than tubulin. To address the former possibility, we designed mass spectrometric approaches for identifying the tubulyzines' binding site. Two strategies were

*Abbreviations:* MS-DRC, mass spectrometric measurement of the differential reactivity of cysteines; mBrB, monobromobimane; GTP, guanosine-5'-triphosphate; rt, room temperature; LC-MS, liquid chromatography-mass spectrometry; THF, tetrahydrofuran; DIPEA, diisopropylethylamine; EtOAc, ethyl acetate; TEA, triethylamine; T-LC, thin-layer chromatography; PIPES, piperazine-*N,N*-bis(ethanesulfonic acid); TCEP, tris(2-carboxyethyl)phosphine hydrochloride; Tn, tubulyzine affinity derivatives; ESI, electrospray ionization; HPLC, high-performance liquid chromatography; CID, collision induced dissociation; MS, mass spectrometry; SIC, single ion current; TIC, total ion current; FWHM, full width at half maximum; GDP, guanosine di phosphate; TA, tubulyzine A; TB, tubulyzine B.

*Keywords:* Tublin; Tubulyzine; Binding site; MS-DRC.

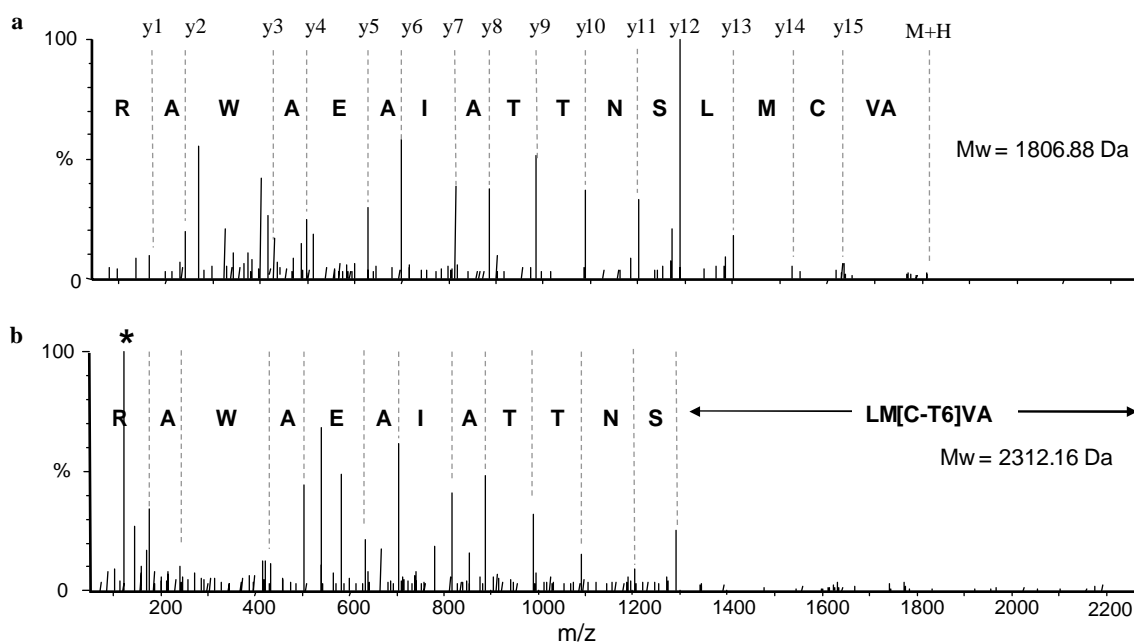
\* Corresponding author. Tel.: +1 212 998 8491; fax: +1 212 260 7905; e-mail: [yt.chang@nyu.edu](mailto:yt.chang@nyu.edu)

† Present address: Aptanomics, 181-203 Ave Jean Jaures, 69001 Lyon, France.



**Table 1.** Cysteine-containing peptides resulting from the trypsin digestion of the  $\alpha\beta$ -tubulin heterodimer

Residue	Sequence	$M_w$	Probing Cys
$\beta$ : 3–19	EIVHIQAGQC <u>GN</u> QIGAK	1764.89	12Cys
$\beta$ : 123–154	ESE <u>SCD</u> CLQGFQLTHSLGGGTGSGMGTLLISK	3212.48	127, 129Cys
$\beta$ : 175–213	VSDTVVEPYNATLSVHQLVENTDETY <u>CID</u> NEALYDI <u>CFR</u>	4478.06	201, 211Cys
$\beta$ : 217–241	LTTPTYGDLNHLVSATMSGVTT <u>CLR</u>	2650.31	239Cys
$\beta$ : 298–306	NIMMA <u>ACD</u> PR	1007.40	303Cys
$\beta$ : 351–359	TAV <u>CD</u> IPPR	970.49	354Cys
$\alpha$ : 3–40	ECISIHVGQAGVQIGNAC <u>WELYC</u> LEHGIQPD <u>SQ</u> MPSDK	4124.89	4, 20, 25Cys
$\alpha$ : 125–156	LADQCTGLQGFVLFHSGGGTGS <u>GFTS</u> LLMER	3332.60	129Cys
$\alpha$ : 167–214	LEFSIYPAPQVSTAVVEPYNSILTHTTLEHSD <u>CAF</u> MVDNEAIYDI <u>CFR</u>	5402.55	200, 213Cys
$\alpha$ : 281–304	AYHEQLSVAEITNAC <u>FEPAN</u> QMVK	2692.26	295Cys
$\alpha$ : 305–308	<u>CD</u> PR	489.20	305Cys
$\alpha$ : 312–320	YMA <u>CC</u> LLYR	1134.50	315, 316Cys
$\alpha$ : 340–352	TIQFVDW <u>CPT</u> GFK	1540.74	347Cys
$\alpha$ : 374–390	AV <u>CML</u> SNTTAAEAWAR	1806.88	376Cys

**Figure 3.** MS/MS spectra of one of the cysteine-containing peptides (a) and its T6-modified form (b). Intensities of the  $y$ -series ions of the T6 modified peptide were reduced with a strong  $p$ -methoxybenzyl ion at 121.1 Da indicated with an asterisk.

the peptides, the intensity of the  $y$ - and  $b$ -series ions in the MS/MS spectrum decreased dramatically along with the increasing intensity of the  $p$ -methoxybenzyl ion released from tubulyzine during fragmentation. The partial loss of the  $y$ -series ions and the reduction of the total fragment ion signals were due to the stable  $p$ -methoxybenzyl ion (121.1 Da) that neutralizes other protonated peptide fragments. Although this event decreases the coverage of amino acid sequencing, the strong peak at 121.1 Da provides a unique signature for tubulyzine modification, which confirms identification.

Once we identified all the cysteine-containing peptides and their Tn-modified forms, the ion intensities were quantified. Since modification of the Tn to the peptide introduces an additional protonation site at the triazine ring, the charge state of the Tn-modified peptides in the mass spectra is higher than that of the corresponding

unmodified peptides. Therefore, we added all the possible charge states together in the calculation. The reaction yield of each cysteine toward Tn was calculated from Eq. 1. Figure 4 shows the relative reaction yield of each cysteine toward the tubulyzine derivatives T6 and T7, which are 5–10 times weaker than tubulyzines, but still active tubulin inhibitors. We found that nine peptides were modified in the T6 experiment and seven peptides were modified in the T7 experiment. In both data sets, the reactivity profiles of the cysteines (across 14 peptides) look very similar, and the most reactive cysteine in  $\beta$ -tubulin was 12Cys in both the T6 and T7 experiments. However, in  $\alpha$ -tubulin, 376Cys shows reactivity similar to 12Cys $\beta$ .

Although the reactivity seen was assumed to be predominantly driven by the specific binding of tubulyzine, a general alkylating reaction as a result of non-specific binding could possibly contribute to the final reaction

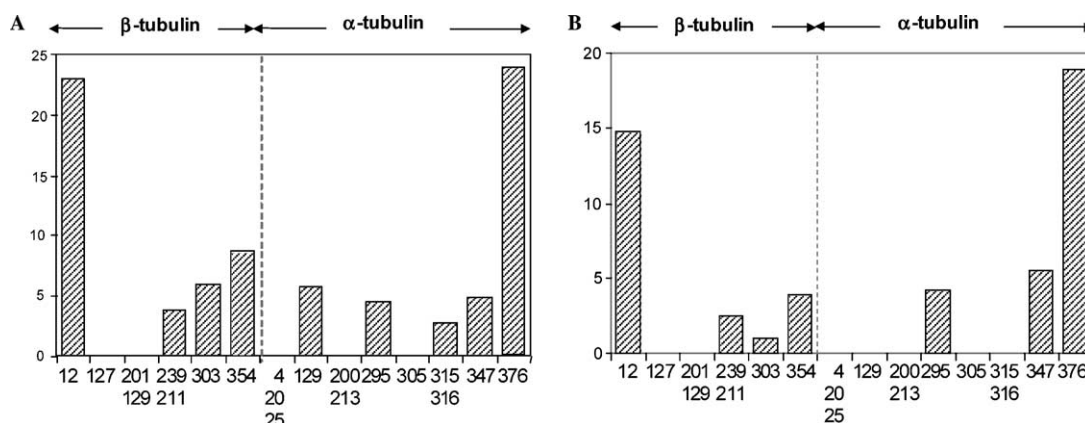


**Figure 4.** Relative reactivity of cysteines toward (A) T6 and (B) T7. In both cases, 12Cys in the  $\beta$  and 376Cys in the  $\alpha$ -tubulin showed the greatest reactivity.

yield. Thus, the reaction of Tn to cysteines which are not near the original tubulyzine binding site remains a possible problem. This is one of the drawbacks of the traditional chemical affinity labeling approach.<sup>12</sup> However, it is notable in this regard that most of the peptides labeled by T6 and T7 contain cysteine residues previously shown to be the most reactive to a number of general sulfhydryl reactive probes, including iodoacetamide and *N*-ethylmaleimide. These residues are 239 and 354 in  $\beta$ -tubulin, and 315, 316, 347, and 376 in  $\alpha$ -tubulin.<sup>11</sup> Thus, the major site of the reaction of T6 and T7 with tubulin, aside from the non-specifically reactive residues, is at 12Cys $\beta$ .

## 2.2. Identification of the tubulyzine binding site using the MS-DRC method

Since the MS-DRC method does not require any structural modification to the drugs, a series of tubulyzines (TA and TB) were used directly in this study. Figure 5 shows the reaction yield change of each cysteine toward mBrB before and after TA treatment. Noticeable reactivity changes at 12Cys $\beta$  and 239Cys $\beta$  were found in this data set.

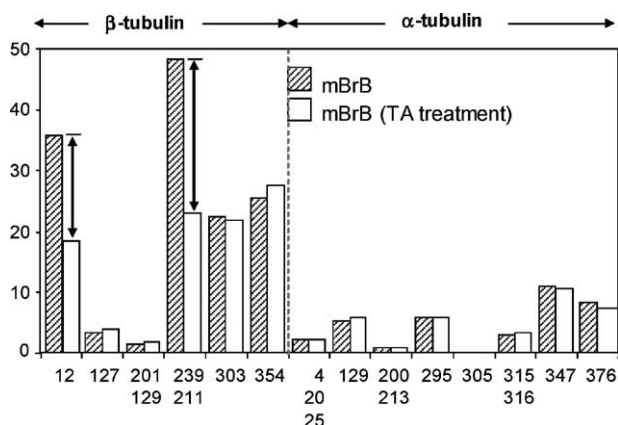


**Figure 5.** Relative reactivities of each cysteine toward mBrB with and without TA pretreatment. The reactivity of mBrB decreased at 12Cys and 239Cys in  $\beta$ -tubulin after TA treatment.

Primarily, any reactivity reduction is due to the occupancy of a drug that blocks the alkylation reaction. Therefore, a cysteine that has differential reactivity before and after drug treatment can be considered as a probable drug-binding site. Previous MS-DRC experiments demonstrated two categories of known tubulin-binding agents: (1) those agents for which the largest reduction of reactivity occurred at 239Cys $\beta$ , such as colchicine, podophyllotoxin, and 2-methoxyestradiol, and (2) those agents for which the largest reduction of reactivity occurred at 12Cys $\beta$ , such as GDP,<sup>13</sup> and cryptophycin and vincristine (unpublished data). In no case did any of these tubulin targeting agents show a dual decrease at both 12Cys $\beta$  and 239Cys $\beta$  as was the case for tubulyzine.

The second source of reactivity reduction could possibly arise from a conformational change in the target protein. Previous studies have suggested that colchicine binding at tubulin causes a conformational change in tubulin<sup>14</sup> and the MS-DRC study demonstrated that pretreatment with colchicine decreased the reactivity at 239Cys $\beta$  and increased the reactivity at 12Cys $\beta$ . This increased reactivity is due to enhanced vulnerability after the conformational change. Therefore, the dual-site reactivity changes seen after tubulyzine treatment may demonstrate a possible conformational change in tubulin.

Interestingly, a similar MS-DRC result was found when comparing the free dimer form of tubulin with the microtubule form.<sup>13</sup> The reactivity of the cysteines in the free dimer form was reduced upon formation of the microtubule. The largest reduction of reactivity was shown at both Cys12 and Cys239 in  $\beta$ -tubulin. The reduction at Cys12 $\beta$  is due to the occupancy of the GDP site as well as its burial in the polymer form, and the reduction at Cys239 $\beta$  may possibly be explained by the restricted accessibility of mBrB toward Cys239 $\beta$  due to the more rigid structure of tubulin in the polymer form.

Cys239 $\beta$  is a very reactive cysteine that binds with various tubulin targeting agents including T13067 developed

by Tularik Inc.<sup>15</sup> Since the Cys239 $\beta$  is not located on the surface of tubulin, its distinctive reactivity is intriguing.<sup>9,16</sup> One possibility is that its higher reactivity may be due to the higher accessibility and/or a lower  $pK_a$  of its thiol.<sup>11</sup> However, it has been speculated that tubulin's dynamic structural change (semi-folding and unfolding equilibrium) may allow the agent access to the inside of tubulin. Therefore, once it forms a rigid structure in the microtubule form, tubulin may no longer open up, and the accessibility toward 239Cys $\beta$  can be reduced. This hypothesis explains the large reactivity reduction at Cys239 $\beta$  seen following microtubule formation.

Therefore, the dual reduction of reactivity using tubulyzine may indicate that the tubulyzines bind to 12Cys $\beta$  and their binding inhibits the opening of the tubulin structure. This then leads to the reactivity reduction in 239Cys $\beta$ . Additionally, 12Cys $\beta$  is known to be a part of the exchangeable GTP-binding site<sup>14,17</sup> and has been suggested as playing an important role in the structure and function of tubulin.<sup>18</sup> Figure 6 shows the computational modeling of T6 resting at a GDP-binding pocket of  $\beta$ -tubulin.

The 12Cys $\beta$  binding site result from MS-DRC overlaps with the previous result from the chemical affinity experiment. The reactivity change seen at 376Cys $\alpha$  was not significant enough to consider in this study. The results obtained following pretreatment with TB were the same (results not shown).

Using the previously identified tubulyzines and their chemical affinity derivatives, we undertook a two pronged approach to identify the binding site of tubulin. Based on our mass spectrometric binding studies using both chemical affinity and MS-DRC, we conclude that the binding site of tubulyzine on the tubulin dimer is 12Cys $\beta$ . This information illuminates the nature of the tubulyzines' activity, while also providing important

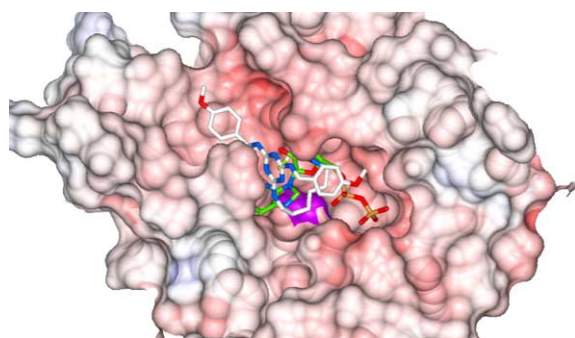


**Figure 6.** Predicted conformation of T6 docked at the C12 site of the tubulin GDP binding pocket. Docked T6 (white) superimposed with the crystal structure of bound GDP (green).<sup>9</sup> The model predicts that a methoxy-phenyl moiety of T6 (top left) occupies a side cavity next to the GDP binding pocket generated by side-chain rearrangements of the tubulin surface residues. This pharmacophoric feature could guide further optimization of high affinity ligands. The molecular surface representation of tubulin is colored by its electrostatic potential (red, electronegative; gray, hydrophobic). T6/GDP color coding is carbon, white/green; oxygen, red; and nitrogen, blue. Cys12 is colored as violet.

structural information for the rational design of future tubulin targeting compounds and second generation tubulyzines.

### 3. Experimental procedures

#### 3.1. Synthesis of tubulyzine affinity molecules

Unless otherwise noted, materials and solvents were obtained from commercial suppliers (Acros and Aldrich) and were used without further purification. Analytical thin-layer chromatography was conducted on SAI F<sub>254</sub> precoated silica gel plates (250  $\mu$ m layer thickness). Chromatography was performed on Sorbent Technologies silica gel, 60 (63–200 mesh). All compounds were identified by an LC–MS at 250 nm (Agilent Technology, HP1100) using a C18 column (20  $\times$  4.0 mm) with a gradient of 5–95% CH<sub>3</sub>CN–H<sub>2</sub>O (containing 0.1% acetic acid) as an eluent over 4 min. <sup>1</sup>H NMR spectra were measured on a Bruker AV-400 MHz spectrometer.

**3.1.1. Synthesis of 2-chloro-4,6-di(4-methoxybenzylamino)-1,3,5-triazine.** This procedure was adapted from US Patent # 6,169,086.<sup>8</sup> A suspension of cyanuric chloride (925 mg, 5.0 mmol) in acetone (10 mL) was cooled on ice and treated dropwise with 4-methoxybenzylamine (1.29 mL, 9.87 mmol). After the mixture was stirred at that temperature for 10 min, 10 mL of a 1 N sodium hydroxide aqueous solution was added thereto dropwise at rt, followed by stirring at rt for 15 h. The precipitate was collected by filtration and washed with H<sub>2</sub>O, diethyl ether, and hexane to obtain the product as a white solid. Sixty to seventy percent yield liquid chromatography–mass spectrometry (LC–MS) ( $m/z$ ) calculated for C<sub>19</sub>H<sub>20</sub>ClN<sub>5</sub>O<sub>2</sub>: 385.13. Found: 386.1 [M+H]<sup>+</sup>.

**3.1.2. Synthesis of 2-(1,6-hexanediamine)-4,6-di(4-methoxybenzylamino)-1,3,5-triazine.** To a solution of 2-chloro-4,6-di(4-methoxybenzylamino)-1,3,5-triazine (100 mg, 0.25 mmol) and 1,6-hexanediamine (189  $\mu$ L, 1.3 mmol) in THF (10 mL) was added DIPEA (270  $\mu$ L, 1.55 mmol). The solution was heated at 70  $^{\circ}$ C for 3 h in a heating block and the solvent was removed by vacuum filtration. The compound was isolated by column chromatography in 50/50 ethyl acetate (EtOAc)/MeOH with 1% triethylamine (TEA)  $R_f$  = 0.267. LC–MS ( $m/z$ ) calculated for C<sub>25</sub>H<sub>35</sub>N<sub>7</sub>O<sub>2</sub>: 465.29. Found: 466.1 [M+H]<sup>+</sup>.

**3.1.3. Synthesis of 2-(4,7,10-trioxa-1,13-tridecanediamine)-4,6-di(4-methoxybenzylamino)-1,3,5-triazine.** To a solution of 2-chloro-4,6-di(4-methoxybenzylamino)-1,3,5-triazine (100 mg, 0.259 mmol) and of 4,7,10-trioxa-1,13-tridecanediamine (285  $\mu$ L, 1.3 mmol) in THF (10 mL) was added DIPEA (270  $\mu$ L, 1.554 mmol). The solution was heated at 70  $^{\circ}$ C for 3 h in a heating block, The solvent was removed by vacuum filtration. The compound was isolated by silica column chromatography in 50/50 EtOAc/MeOH with 1% TEA.  $R_f$  = 0.4 LC–MS ( $m/z$ ) calculated for C<sub>29</sub>H<sub>43</sub>N<sub>7</sub>O<sub>5</sub>: 569.33. Found: 570.2 [M+H]<sup>+</sup>.

**3.1.4. Synthesis of T6.** To a solution of 2-(1,6-hexanediamine) 4,6-di(4-methoxybenzylamino)-1,3,5-triazine (50 mg, 107  $\mu\text{mol}$ ) in THF (5 mL) was added chloroacetyl chloride (12.9  $\mu\text{L}$ , 162  $\mu\text{mol}$ ) with pyridine (12.9  $\mu\text{L}$ ) in an ice bath with stirring and allowed to rise to rt after the addition. The reaction proceeded for 60 min and was monitored by TLC. The compound was purified by prep-TLC in EtOAc.  $R_f = 0.24$ ;  $^1\text{H NMR}$  ( $\text{CDCl}_3$ )  $\delta$  (ppm) 7.220 (d,  $J = 8.0$ , 4H), 6.829 (d,  $J = 8.4$ , 4H) 4.499 (s, 2H), 4.132 (s, 2H), 3.760 (s, 6H), 3.589 (m, 2H), 3.299 (m, 2H), 1.539–1.738 (m, 4H), 1.256–1.432 (m, 4H). LC–MS ( $m/z$ ) calculated for  $\text{C}_{26}\text{H}_{34}\text{ClN}_7\text{O}_3$ : 541.26. Found: 542.26  $[\text{M}+\text{H}]^+$ .

**3.1.5. Synthesis of T7.** To a solution of 2-(4,7,10-trioxo-1,13-tridecanediamine)-4,6-di(4-methoxybenzylamino)-1,3,5-triazine (50 mg, 87  $\mu\text{mol}$ ) in THF (5 mL) was added chloroacetyl chloride (10.5  $\mu\text{L}$ , 132  $\mu\text{mol}$ ) with pyridine (10.5  $\mu\text{L}$ ) in an ice bath with stirring and allowed to rise to rt after the addition. The reaction proceeded for 30 min and was monitored by TLC. The compound was purified by prep-TLC in EA/10% MeOH.  $R_f = 0.53$ ;  $^1\text{H NMR}$  ( $\text{CDCl}_3$ )  $\delta$  (ppm) 7.205–7.216 (d,  $J = 8.0$ , 4H) 6.816–6.838 (d,  $J = 8.8$ , 4H), 4.483 (s, 4H), 4.082 (s, 2H), 3.782 (s, 6H), 3.515–3.658 (m, 12H), 1.762–1.856 (m, 4H). LC–MS ( $m/z$ ) calculated for  $\text{C}_{31}\text{H}_{44}\text{ClN}_7\text{O}_6$ : 645.3. Found: 646.4  $[\text{M}+\text{H}]^+$ .

## 3.2. Reaction of tubulin with tubulyzine derivatives

Rat brain tubulin was purified from microtubule protein<sup>19</sup> by differential polymerization as previously described.<sup>20</sup> Ten micromole rat brain tubulin in PIPES buffer (50 mM piperazine-*N,N*-bis(ethanesulfonic acid), 0.5 mM  $\text{MgCl}_2$ , pH 7.0) was incubated with 50  $\mu\text{M}$  T6. After incubation, the reaction was quenched by the addition of acetic acid 0.2% (v/v). The protein was immediately precipitated by the addition of 9 vol of  $-20^\circ\text{C}$  acetone. The sample was held at  $20^\circ\text{C}$  for 15 min, centrifuged at 15,000g for 5 min, and all excess reagents were removed. The precipitated tubulin was resolubilized using sonication in 100 mM ammonium bicarbonate buffer solution, pH 7.7, with a bath sonifier. Disulfide bonds, which might be formed after destruction of the tertiary structure of tubulin, were reduced by 1 Tris(2-carboxyethyl)phosphine hydrochloride (TCEP). Additionally, 10% acetonitrile was added for extended denaturation. The protein was digested with sequence-grade modified trypsin (20:1 w/w) for 15 h at  $37^\circ\text{C}$ . Then, 5 mM TCEP was added to ensure complete reduction of the disulfide bonds after digestion. 2-Mercaptoethanol has been widely used as a quenching agent for sulfhydryl reaction, but it was avoided in this study since 2-mercaptoethanol binds not only to the tubulyzine affinity derivatives (Tn) but also to cysteines resulting in a 76 Da molecular weight increase and retention time change during the HPLC separation, which may lead to less accurate quantification due to the splitting and complexity of peaks.

## 3.3. High-performance liquid chromatography and MS

A CapLC-coupled Q-TOF2 mass spectrometer (Waters, Beverly, MA, USA) equipped with an electrospray ionization (ESI) source was used for HPLC–MS analysis. A 100-min high-performance liquid chromatography (HPLC) method was used with a gradient 5% solvent A (0.2% formic acid in aqueous solution) to 90% solvent B (0.2% formic acid in acetonitrile) gradient. A C18 column (300  $\text{\AA}$ ,  $0.32 \times 150$  mm, Microtech Scientific, Vista, CA, USA) and a C18 precolumn (Waters) were used for the separation. A flow rate of 6  $\mu\text{L}/\text{min}$  was used in the HPLC pump, and a 6:1 splitter resulted in a 1 mL/min flow rate at the electrospray. Each sample was subjected to HPLC–MS twice. A tandem mass spectrometry (MS/MS) mode was used in the first run to identify all peptides using collision-induced dissociation (CID)-based peptide sequencing. Once all the peptides and modified peptides were identified, a subsequent full-scan MS mode was used in the second run to quantify the modified and unmodified cysteine-containing peptide pairs.

## 3.4. Reaction for differential reaction yield study

Tubulin was incubated with 50  $\mu\text{M}$  unmodified tubulyzine for 20 min at  $37^\circ\text{C}$  to form the protein–ligand complex. The solution was then incubated with 50  $\mu\text{M}$  mBrB and processed as above.

**3.4.1. Data analysis.** Tryptic digestion generates 14 cysteine-containing peptides from the major form of brain tubulin dimer as shown in Table 1. Each peptide and its modified entity were identified based on sequence information obtained by the MS/MS experiment. The retention time and molecular weight of each identified peptide were then used for identification in the liquid chromatography LC–MS data of the second run. A single ion current (SIC) chromatogram of each ion pair (cysteine-containing peptide ion and modified cysteine-containing peptide ion) was reconstituted to extract a selected signal that originates from the particular peptide of interest from the total ion current (TIC) chromatogram, as shown in Figure 2. The  $m/z$  extraction range was determined by taking the full width at half maximum (FWHM) of the most abundant isotope peak ( $m/z \pm 0.5$  FWHM) of each ion. Extracting only the single isotope peak enhances the accuracy of quantitation by eliminating the involvement of highly overlapped peaks. Each peak area of the SIC chromatogram constructed by this method was integrated using built-in software (MassLynx 4.0, Waters Corporation) to calculate the intensity of each peak. Reactivity yields were calculated by dividing the intensity of the modified peptide by the overall intensity:

$$\text{Reactivity} = 100 \times [I_M / (I_U + I_M)], \quad (1)$$

where  $I_U$  and  $I_M$  are intensities of the unmodified peptide and modified peptide, respectively.

**3.4.2. Computational study.** T6 was docked to the guanosine diphosphate (GDP) binding pocket of tubulin with ICM (Molsoft LLC, San Diego, CA). Hydrogen was

added to the crystal structure of the tubulin–GDP complex (PDB code 1jff)<sup>9</sup> and GDP was removed. T6 was placed at random in the GDP pocket, and the energy of the system was extensively minimized by a Biased Probability Monte Carlo simulation (the conformational space was sampled by 2,570,000 Monte Carlo steps) in the internal coordinates, space<sup>10</sup> with a flexible ligand and flexible receptor side chains within 12 Å of bound GDP. Three independent runs with differing starting conformations converged towards the final model.

### Acknowledgments

Y.T.C. is grateful for financial support from NIH (R01 CA096912) and thanks the National Science Foundation for equipment grants for the NMR (MRI-0116222) and the Capillary LC-Ion Trap Mass spectrometer (CHE-0234863). Components of this work were conducted in a Shared Instrumentation Facility constructed with support from Research Facilities Improvement Grant C06 RR-16572 from the NCI/NIH.

### References and notes

1. Vilpo, J. A.; Koski, T.; Vilpo, L. M. *Eur. J. Haemato.* **2000**, *65*, 370.
2. Smith, C. D.; Zhang, X. *J. Biol. Chem.* **1996**, *271*, 6192.
3. Poirier, V. J.; Hershey, A. E.; Burgess, K. E.; Phillips, B.; Turek, M. M.; Forrest, L. J.; Beaver, L.; Vail, D. M. *J. Vet. Intern. Med.* **2004**, *18*, 219.
4. Tinwell, H.; Ashby, J. *Carcinogenesis* **1994**, *15*, 1499.
5. Rosania, G. R.; Chang, Y. T.; Perez, O.; Sutherlin, D.; Dong, H.; Lockhart, D. J.; Schultz, P. G. *Nat. Biotechnol.* **2000**, *18*, 304.
6. Perez, O. D.; Chang, Y. T.; Rosania, G.; Sutherlin, D.; Schultz, P. G. *Chem. Biol.* **2002**, *9*, 475.
7. Moon, H. S.; Jacobson, E. M.; Khersonsky, S. M.; Luzung, M. R.; Walsh, D. P.; Xiong, W.; Lee, J. W.; Parikh, P. B.; Lam, J. C.; Kang, T. W.; Rosania, G. R.; Schier, A. F.; Chang, Y. T. *J. Am. Chem. Soc.* **2002**, *124*, 11608.
8. Ejima, A.; Ohsuki, S.; Ohki, H.; Naito, H. U.S. Patent 6,169,086, 2001.;
9. Lowe, J.; Li, H.; Downing, K. H.; Nogales, E. *J. Mol. Biol.* **2001**, *313*, 1045.
10. Totrov, M.; Abagyan, R. *Proteins Suppl.* **1997**, *1*, 215.
11. Britto, P. J.; Knipling, L.; Wolff, J. *J. Biol. Chem.* **2002**, *277*, 29018.
12. Bai, R.; Pei, X. F.; Boye, O.; Getahun, Z.; Grover, S.; Bekisz, J.; Nguyen, N. Y.; Bossi, A.; Hamel, E. *J. Biol. Chem.* **1996**, *271*, 12639.
13. Kim, Y. J.; Pannell, L. K.; Sackett, D. L. *Anal. Biochem.* **2004**, *332*, 376.
14. Shivanna, B. D.; Mejillano, M. R.; Williams, T. D.; Himes, R. H. *J. Biol. Chem.* **1993**, *268*, 127.
15. Shan, B.; Medina, J. C.; Santha, E.; Frankmoelle, W. P.; Chou, T. C.; Learned, R. M.; Narbut, M. R.; Stott, D.; Wu, P.; Jaen, J. C.; Rosen, T.; Timmermans, P. B.; Beckmann, H. *Proc. Natl. Acad. Sci. U.S.A.* **1999**, *96*, 5686.
16. Nogales, E. *Annu. Rev. Biophys. Biomol. Struct.* **2001**, *30*, 397.
17. Luduena, R. F.; Roach, M. C. *Pharmacol. Ther.* **1991**, *49*, 133.
18. Gupta, M. L., Jr.; Bode, C. J.; Dougherty, C. A.; Marquez, R. T.; Himes, R. H. *Cell Motil. Cytoskeleton* **2001**, *49*, 67.
19. Sackett, D. L.; Knipling, L.; Wolff, J. *Protein Expr. Purif.* **1991**, *2*, 390.
20. Wolff, J.; Sackett, D. L.; Knipling, L. *Protein Sci.* **1996**, *5*, 2020.